Phases of deformation in filament networks with active cross-link slip

William McFadden, Edwin Munro

University of Chicago, Institute for Biophysical Dynamics, Chicago, IL 60615

(Dated: this day)

Abstract

CONTENTS

I. INTRODUCTION

II. EXPLANATION OF MODEL

A. Composite Cross-link & Filament Representation

We consider individual filaments as chains of springs with relaxed length l_s. The orientations of neighboring springs are linearly coupled. Filaments can therefore be represented as a sequence of nodes with positions $\mathbf{x_i}$ and nearest neighbor interactions of the form

$$|F_{i,i+1}|_{\parallel} = -\mu \cdot \frac{|\mathbf{x_{i+1}} - \mathbf{x_i}| - l_s}{l_s} \tag{1}$$

$$|F_{i,i+2}|_{\perp} = -\frac{\kappa}{l_s^2} \cdot acos\left(\frac{\mathbf{x_{i+2}} - \mathbf{x_{i+1}}}{|\mathbf{x_{i+2}} - \mathbf{x_{i+1}}|} \cdot \frac{\mathbf{x_{i+1}} - \mathbf{x_i}}{|\mathbf{x_{i+1}} - \mathbf{x_i}|}\right) \tag{2}$$

where, μ represents an extensional modulus of a filament, and κ represents a bending modulus. This is essentially a discretized equivalent to a model of filaments with separable extensional and bending moduli as in [17]. We define the totally elastic force on a node as

$$\nabla \mathcal{H}_i = |F_{i,i+1}|_{\parallel} + |F_{i,i+2}|_{\perp} \tag{3}$$

Here, we take the extensional modulus as a composite quantities related to both filament and cross-linker compliance in a manner similar to a recently proposed effective medium theory[4]. In the limit of highly rigid cross-links and flexible filaments, our model reduces to the pure semi-flexible filament models of [17, 45]. In the opposite regime of nearly rigid filaments and highly flexible cross links, our method is still largely similar to the model of [4] in small strain regimes before any nonlinear cross link stiffening. However, in departure from those models, the magnitude of the force on interior cross-links in our model is still the same as those on the exterior. This is a simplification of the varying levels of strain that would actually be present in these cross-linkers as addressed in [4], but we choose to ignore the slight variation in favor of an approximated, global mean approach.

B. 2D Network Formation

We choose to focus our attention on 2D networks both for their tractability as well as their relevance in the quasi-2D cytoskeletal cortex of many eukaryotic cells[31]. In addition, recent developments in 2D *in vitro* systems[34, 36], make 2D models all the more interesting as a renewed focus of study.

We follow a mikado model approach by initializing a minimal network of connected unstressed linear filaments in a rectangular 2D domain. We generate 2D networks of these semi-flexible filaments by laying down straight lines of length, L, with random position and orientation. We then assume that some fixed fraction of overlapping filaments become cross-linked (defined in II C) at their point of overlap.

Although real cytoskeletal networks may form with non-negligible anisotropy, we focus on isotropically initialized networks for simplicity. We define the density using the average distance between cross-links along a filament, l_c. A simple geometrical argument can then be used to derive the number of filaments filling a domain as a function of L and l_c[17]. Here, we use the approximation that the number of filaments needed to tile a rectangular domain of size $W \times H$ is $2WH/Ll_c$, and that the length density is therefore $1/l_c$.

In the absence of cross-link slip, we expect the network to form a connected solid with a well defined elastic modulus[17, 45]. These networks are only well-connected when the ratio of filament length to intercross-link spacing, L/l_c, is greater than ~ 6. Near this percolation threshold, there are only locally connected domains, and discussions of global network properties becomes less reasonable. Additionally, as the filament density is increased beyond this point, there is another transition between non-affine bending and affine stretching of filaments, which changes the dominating term of the network's elastic modulus.

C. Drag-like Coupling Between Overlapping Filaments

In contrast to previous models, we allow relaxation of the network's stored stress by letting the attachment points slip. We do this by replacing an elastic interaction between pairs of points along filaments with a drag-like coupling between filaments.

$$\mathbf{F_{drag}} = \xi \cdot \int ds \, (\mathbf{v_i}(\mathbf{s}) - \mathbf{v_j}(\mathbf{s})) \, p_{ij}(s) \tag{4}$$

Where $p_{ij}(s)$ represents the locational distribution of cross-link points (equal to 1 at locations of cross-links and 0 elsewhere) and $\mathbf{v_i}(\mathbf{s})$ and $\mathbf{v_j}(\mathbf{s})$ represent the the velocities of the ith and jth filaments. This model assumes a linear relation between applied force and the velocity difference between attached filaments. Obviously, non-linearities can arise in the presence of force dependent detachment kinetics as well as non-linear force extension of cross-links. We address non-linear effects of stress induced unbinding in Appendix A. Assuming inhomogeneities from non-linear effects are of second order, the motion for the entire network is governed by a dynamical equation of the form

$$\int ds \, (\zeta \mathbf{v_i}(\mathbf{s}) + \xi \sum_j (\mathbf{v_i}(\mathbf{s}) - \mathbf{v_j}(\mathbf{s})) \, p_{ij}(s)) = \nabla \mathcal{H}_i \tag{5}$$

Here, the first term in the integral is the filament's intrinsic drag through its embedding fluid, ζ, while the second comes from the drag-like coupling between filaments, ξ.

D. System of Equations for Applied Stress

We model our full network as a coupled system of differential equations satisfying 5. Although the general mechanical response of this system may be very complex, we focus our attention on low frequency deformations and the steady-state creep response of the system to an applied stress. To do this we introduce a fixed stress, σ along the midline of our domain. This stress points in the direction, $\hat{\mathbf{u}}$, producing either shear ($\hat{\mathbf{u}} = \hat{\mathbf{x}}$) or extensional ($\hat{\mathbf{u}} = \hat{\mathbf{y}}$) stress.

Finally, we add a 0 velocity constraint at the far edges of our domain of interest. We assume that our network is in the "dry," low Reynold's number limit, where inertial effects are so small that we can equate our total force to 0. Therefore, we have a dynamical system of wormlike chain filaments satisfying

$$\int ds \left(\zeta \mathbf{v_i}(\mathbf{s}) + \xi \sum_j (\mathbf{v_i}(\mathbf{s}) - \mathbf{v_j}(\mathbf{s}))\, p_{ij}(s)\right) = \nabla \mathcal{H}_i + \sigma \mathbf{u}\hat{(\mathbf{x})} \tag{6}$$

subject to constraints such that $\mathbf{v_i}(\mathbf{x})$ is 0 with $x = 0$. This results in an implicit differential equation for filament segments which can be discretized and integrated in time to produce a solution for the motion of the system.

E. Incorporating Activity at Cross-link Points

Discuss the modifications to the equations to add a motile force at points of overlap.

F. Generating Activity Gradients

III. RESULTS

A. Steady-state Approximation of Effective Viscosity

We begin with a calculation of a strain rate estimate of the effective viscosity for a network described by our model in the limit of highly rigid filaments. We carry this out by assuming

we have applied a constant stress along a transect of the network. With moderate stresses, we assume the network reaches a steady state affine creep. In this situation, we would find that the stress in the network exactly balances the sum of the drag-like forces from cross-link slip. So for any transect of length D, we have a force balance equation.

$$\sigma = \frac{1}{D} \sum_{filaments} \sum_{crosslinks} \xi \cdot (\mathbf{v_i}(\mathbf{x}) - \mathbf{v_j}(\mathbf{x})) \tag{7}$$

where $\mathbf{v_i}(\mathbf{x}) - \mathbf{v_j}(\mathbf{x})$ is the difference between the velocity of a filament, i, and the velocity of the filament, j, to which it is attached at the cross-link location, $\mathbf{x}$. We can convert the sum over cross-links to an integral over the length using the average density of cross-links, $1/l_c$ and invoking the assumption of (linear order) affine strain rate, $\mathbf{v_i}(\mathbf{x}) - \mathbf{v_j}(\mathbf{x}) = \dot{\gamma} x$. This results in

$$\sigma = \frac{1}{D} \sum_{filaments} \int_0^L \xi \cdot \left(\mathbf{v_i}(\mathbf{s}) - \mathbf{v_j}(\mathbf{s})\right) \frac{ds \cos\theta}{l_c}$$
$$= \sum_{filaments} \frac{\xi \dot{\gamma} L}{l_c} \cos\theta \cdot (x_l + \frac{L}{2} \cos\theta) \tag{8}$$

Here we have introduced the variables x_l, and θ to describe the leftmost endpoint and the angular orientation of a given filament respectively. Next, to perform the sum over all filaments we convert this to an integral over all orientations and endpoints that intersect our line of stress. We assume for simplicity that filament stretch and filament alignment are negligible in this low strain approximation. Therefore, the max distance for the leftmost endpoint is the length of a filament, L, and the maximum angle as a function of endpoint is $\arccos(x_l/L)$. The linear density of endpoints is the constant $D/l_c L$ so our integrals can be rewritten as this density over x_l and θ between our maximum and minimum allowed bounds.

$$\sigma = \frac{1}{D} \int_0^L dx_l \int_{-\arccos(\frac{x_l}{L})}^{\arccos(\frac{x_l}{L})} \frac{d\theta}{\pi} \frac{\xi \dot{\gamma} L}{l_c} \cdot \frac{D}{L l_c} \cdot (x_l \cos\theta + \frac{L}{2} cos^2\theta) \tag{9}$$

Carrying out the integrals and correcting for dangling filament ends leaves us with a relation between stress and strain rate.

$$\sigma = \frac{(L - 2l_c)^2 \xi}{4\pi l_c^2} \dot{\gamma} \tag{10}$$

We recognize the constant of proportionality between stress and strain rate as a viscosity. Therefore, our approximation for the effective viscosity, η_{eff}, at steady state creep in this low strain limit is

$$\eta_{eff} = \frac{(L - 2l_c)^2 \xi}{4\pi l_c^2}. \tag{11}$$

As illustrated in Figure 1, under moderate strains ($\gamma < 0.2$), our simulations show that in the high density limit, our theoretical approximation from Eqn 11 is highly accurate at explaining the network behavior. Aside from a geometrical factor, our approximation is valid for both shear and extensional stresses applied to the network.

As the density of the network approaches the breakdown limit, the effective viscosity diverges from our expected value. At the low connectivities, our expected viscosity goes to 0, but the medium viscosity begins to take over as we cross the percolation threshold at $L/l_c \sim 6$.

In addition to changing the architecture and effective drag coefficient, we also validated the generality of our approximation by varying simulation size, medium viscosity, filament stiffness, and applied stress. We were able to find a slight trend that depended on filament stiffness as indicated in the difference between blue and red data points in Figure 1. The deviation from our approximation and variability in results manifested itself more strongly when filaments were highly compliant. To investigate this effect further, we next performed a more detailed analysis of the creep response while varying filament compliances.

IV. SUMMARY AND CONCLUSIONS

We have proposed a simplified effective friction model for understanding 2D cross-linked networks. Our model extends previous Mikado and lattice models to include effects of cross-link relaxation. We expect that our model can confer insights into mechanisms of network stress relaxation in quasi-2D networks such as those found in *in vitro* actin monolayer experiments[34] as well as in eukaryotic actomyosin cortices[31].

Our model is the first to address the plausible dependence of network effective viscosity on network structural properties. This led to a derivation of an estimate for the long timescale creep rate of networks under constant stress. Although this derivation neglects possible frequency dependence at short timescales, this finding offers a potential framework

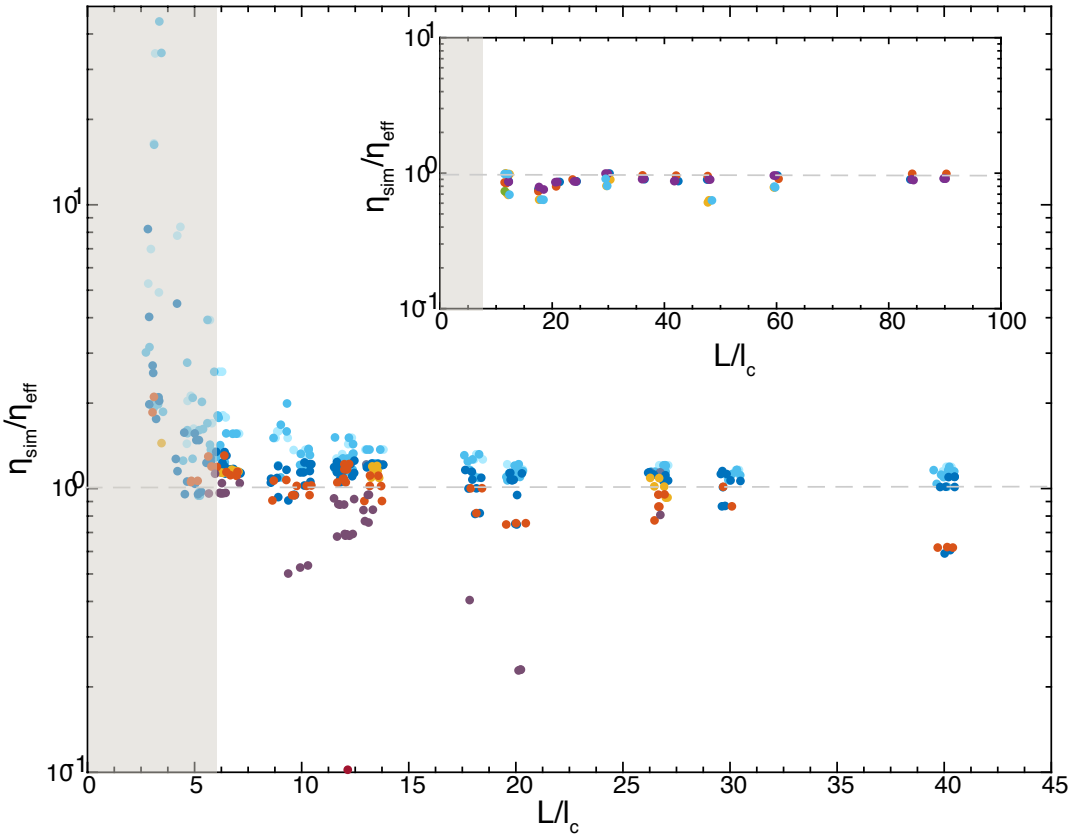

FIG. 1. Ratio of effective viscosity measured by shear simulation to predicted effective viscosity as a function of connectivity, L/l_c. Inset: Same measurement for extensional simulations

for addressing the dependence of network deformation rate on filament concentration and length.

Additionally, our simulations suggest that, in the presence of constant shear stress, cross-link friction will also produce a long-lived phase of sublinear creep as filaments relax from their affine stretched position. While this phase may transiently resemble more explicit 3D models such as [5], it is clear that our model differs by predicting that network will achieve a constant effective viscosity more rapidly. In particular, we predict that this relaxation will occur at a rate similar to that of rate of cross-link slip derived strain and will therefore be negligible after the network has slipped by roughly ten times the magnitude of the purely affine mechanical deformation.

In building our model we have neglected any other sources of potential mechanical relax-

ation in order to simplify out analysis. In the future, we hope to extend our model to include biochemically driven forms of relaxation such as filament turnover or regulated cross-link unbinding.

This model forms a basis for addressing 2D filament network deformation, and it proposes a simplified formulation of important qualitative properties. In this way we are able to address potentially general phases of network deformation and delineate what network properties may give rise to them. This may provide an important starting point for addressing the general importance of network structure in more complex networks containing active elements.

V. ACKNOWLEDGEMENTS

Appendix A: Deriving Molecular Drag Coefficients

Thus far, the idea of a molecular drag coefficient was taken as a phenomenological, measured parameter for a given experimental setup. While this is a sufficient pragmatic justification, it's useful to try to motivate the quantitative value of this drag coefficient by connecting it to the underlying cross-link properties of binding affinity, concentration, and extensibility.

To do this we'll imagine the simplified case of two cross linkers sliding past each other in one dimension. In this case, assume that we have an equilibrium number of bound cross-linkers, n_B, each of which is displaced from its equilibrium length by some distance x. Each cross linker unbinds with rate k_{off} and rebinds at it's relaxed position ($x = 0$) with rate k_{on}. At the same time, all the cross linkers are being pulled from their relaxed position at a rate, v, which is simply the rate at which the filaments are sliding past each other.

We can write the differential equation for the change in the density of cross-links, ρ, at displacement x as they are pulled upon, bind, and unbind.

$$\frac{\partial \rho}{\partial t} = -k_{off}\rho(x) - v\frac{\partial \rho}{\partial x} + k_{on}\delta(x) \tag{A1}$$

Recognizing that $\int \rho(x) = n_B$ implies $k_{on} = k_{off}n_B$, we can find the steady state solution

$$\rho(x) = \frac{n_b k_{off}}{v} \cdot exp\left(-\frac{k_{off}}{v}x\right) \tag{A2}$$

If each cross-link has a spring constant μ_c, then we can equate the force on all cross-links to the applied force that is sliding the filaments past each other. Realistically, the spring constant and binding affinity would be functions of the cross-link stretch, but here we are taking them as approximately constant.

$$\int_0^\infty \rho(x)\mu_c x dx = v\frac{\mu_c n_B}{k_{off}} = F_{app} \tag{A3}$$

a

Therefore, the term next to v, (i.e. $\frac{\mu_c n_B}{k_{off}}$) would be equal to our molecular drag coefficient, ξ. Assuming approximately 1 cross link per filament overlap, and using parameter estimates culled from Ferrer et al., we build the following table of estimates for ξ.

cross-linker type	α-actinin	filamin-A
dissociation constant (s^{-1})	0.4	0.6
spring constant ($nN/\mu m$)	455	820
drag coefficient, ξ ($\frac{nN \cdot s}{\mu m}$)	182	492

This molecular description assumed both a constant off-rate and linear force extension of cross-links. In the event that binding kinetics are regulated by the state of extension, we would expect (based on Rf) to find a region that exhibits a stick-slip behavior instead of the smooth. Depending on the nature of any coupling between cross-links local stick-slip could either give rise to a global stick-slip behavior or a heterogenous mixture of stuck and sliding cross-links. It would be interesting to explore this topic further in the future, but in the present analysis, we choose to ignore complications from these nonlinear effects.

Appendix B: Computational Simulation Method

We tested our analytical conclusions on a computational model. More technical details of the model can be found in the Appendix, but we summarize the main modeling points here.

We discretize the filaments such that the equations of motion becomes a coupled system of equations for the velocities of filament endpoints, $\mathbf{x}$. The drag-like force between overlapping filaments results in a coupling of the velocities of endpoints.

$$\mathbf{A} \cdot \dot{\mathbf{x}} = \mathbf{f}(\mathbf{x}) \tag{B1}$$

where $\mathbf{A}$ represents a coupling matrix between endpoints of filaments that overlap, and $\mathbf{f}(\mathbf{x})$ is the spring force between pairs of filament segment endpoints. We can then numerically integrate this system of equations to find the time evolution of the positions of all filament endpoints.

We generate a network by laying down filaments with random position and orientation within a domain of size $2D$ by D with periodic boundaries in the y-dimension. The external stress (shear or extensional/compressional) is applied to all filament endpoints falling within a fixed x-distance from the center of the domain. Finally, filament endpoints falling within a fixed x-distance from the edges of the domain are constrained to be nonmoving.

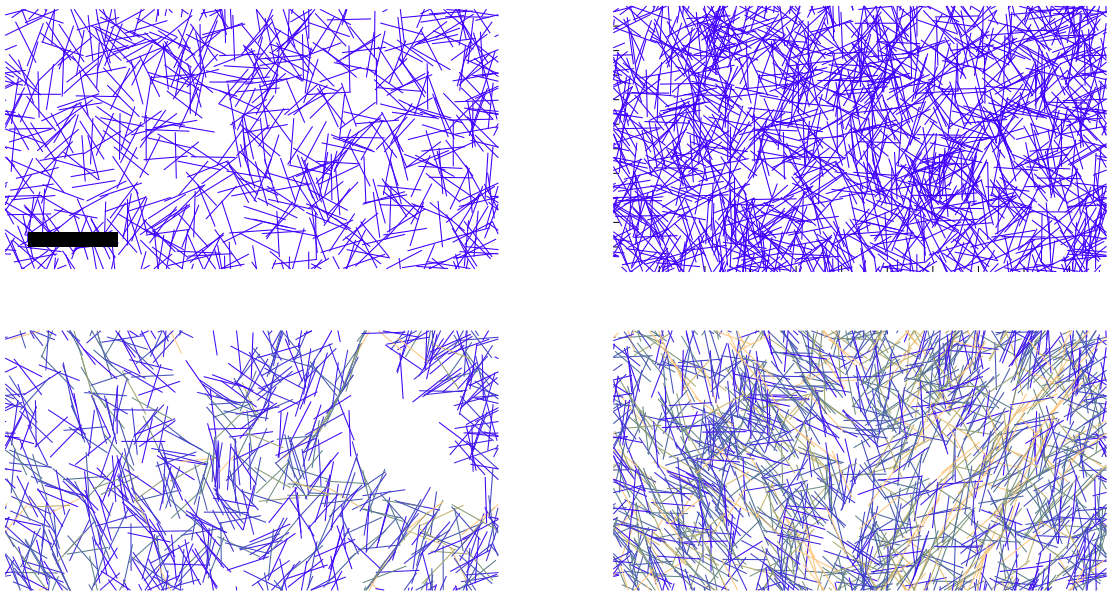

FIG. 2. Two Simulation setups with $L = 9\mu m, D = 54\mu m$ before (top) and after (bottom) 1000 seconds of applied stress. a) low density $l_c = 2\mu m$, b) moderate density $l_c = 1\mu m$. Scale bar $20\mu m$

The nominal units for length, force, and time are μm, nN, and s, respectively. We explored parameter space around an estimate of biologically relevant parameter values, given in Table I.

For computational simplicity in these models, unless otherwise mentioned we assume that the bending rigidity, κ, is infinite. This allows us to model filaments as non-bending springs

TABLE I. Simulation Parameter Values

parameter	**symbol**	**physiological estimate**
extensional modulus	μ	$1nN$
bending modulus	κ	$10^{-3}nN \cdot \mu m$
cross-link drag coefficient	ξ	$unknown$
medium drag coefficient	ζ	$0.0005\frac{nNs}{\mu m^2}$
filament length	L	$5\mu m$
cross-link spacing	l_c	$0.5\mu m$
domain size	D	$10 - 50\mu m$

of rest length, L, and spring modulus μ. In the appendix, we show that our result is not significantly different from the result for semi-flexible polymers.

[1] Shiladitya Banerjee, M. Cristina Marchetti, and Kristian Müller-Nedebock. Motor-driven dynamics of cytoskeletal filaments in motility assays. *Phys. Rev. E*, 84:011914, Jul 2011.

[2] Andreas R. Bausch, Florian Ziemann, Alexei A. Boulbitch, Ken Jacobson, and Erich Sackmann. Local measurements of viscoelastic parameters of adherent cell surfaces by magnetic bead microrheometry. *Biophysical Journal*, 75(4):2038 – 2049, 1998.

[3] D Bray and JG White. Cortical flow in animal cells. *Science*, 239(4842):883–888, 1988.

[4] C. P. Broedersz, C. Storm, and F. C. MacKintosh. Effective-medium approach for stiff polymer networks with flexible cross-links. *Phys. Rev. E*, 79:061914, Jun 2009.

[5] Chase P. Broedersz, Martin Depken, Norman Y. Yao, Martin R. Pollak, David A. Weitz, and Frederick C. MacKintosh. Cross-link-governed dynamics of biopolymer networks. *Phys. Rev. Lett.*, 105:238101, Nov 2010.

[6] P. Broedersz, C. and C. MacKintosh, F.˙Modeling semiflexible polymer networks. *Rev. Mod. Phys.*, 86:995–1036, Jul 2014.

[7] Preethi L. Chandran and Mohammad R. K. Mofrad. Averaged implicit hydrodynamic model of semiflexible filaments. *Phys. Rev. E*, 81:031920, Mar 2010.

[8] Christian J. Cyron, Kei W. Müller, Andreas R. Bausch, and Wolfgang A. Wall. Micromechanical simulations of biopolymer networks with finite elements. *Journal of Computational*

Physics, 244(0):236 – 251, 2013. Multi-scale Modeling and Simulation of Biological Systems.

[9] M. Doi and S. F. Edwards. *The Theory of Polymer Dynamics*. Oxford University Press, USA, November 1986.

[10] Fangming Du, John E. Fischer, and Karen I. Winey. Effect of nanotube alignment on percolation conductivity in carbon nanotube/polymer composites. *Phys. Rev. B*, 72:121404, Sep 2005.

[11] E Evans and A Yeung. Apparent viscosity and cortical tension of blood granulocytes determined by micropipet aspiration. *Biophysical Journal*, 56(1):151–160, 07 1989.

[12] A. E. Filippov, J. Klafter, and M. Urbakh. Friction through dynamical formation and rupture of molecular bonds. *Phys. Rev. Lett.*, 92:135503, Mar 2004.

[13] Daniel A. Fletcher and R. Dyche Mullins. Cell mechanics and the cytoskeleton. *Nature*, 463(7280):485–492, 01 2010.

[14] M. L. Gardel, F. Nakamura, J. Hartwig, J. C. Crocker, T. P. Stossel, and D. A. Weitz. Stress-dependent elasticity of composite actin networks as a model for cell behavior. *Phys. Rev. Lett.*, 96:088102, Mar 2006.

[15] M. L. Gardel, F. Nakamura, J. H. Hartwig, J. C. Crocker, T. P. Stossel, and D. A. Weitz. Prestressed f-actin networks cross-linked by hinged filamins replicate mechanical properties of cells. *Proceedings of the National Academy of Sciences of the United States of America*, 103(6):1762–1767, 2006.

[16] M. L. Gardel, J. H. Shin, F. C. MacKintosh, L. Mahadevan, P. Matsudaira, and D. A. Weitz. Elastic behavior of cross-linked and bundled actin networks. *Science*, 304(5675):1301–1305, 2004.

[17] David A. Head, Alex J. Levine, and F. C. MacKintosh. Deformation of cross-linked semiflexible polymer networks. *Phys. Rev. Lett.*, 91:108102, Sep 2003.

[18] Claus Heussinger, Boris Schaefer, and Erwin Frey. Nonaffine rubber elasticity for stiff polymer networks. *Phys. Rev. E*, 76:031906, Sep 2007.

[19] S N Hird and J G White. Cortical and cytoplasmic flow polarity in early embryonic cells of caenorhabditis elegans. *The Journal of Cell Biology*, 121(6):1343–1355, 1993.

[20] Robert M Hochmuth. Micropipette aspiration of living cells. *Journal of Biomechanics*, 33(1):15 – 22, 2000.

[21] K. E. Kasza, C. P. Broedersz, G. H. Koenderink, Y. C. Lin, W. Messner, E. A. Millman,

F. Nakamura, T. P. Stossel, F. C. MacKintosh, and D. A. Weitz. Actin filament length tunes elasticity of flexibly cross-linked actin networks. *Biophysical Journal*, 99(4):1091–1100, 2015/03/12.

[22] Taeyoon Kim, Wonmuk Hwang, and Roger D Kamm. Dynamic role of cross-linking proteins in actin rheology. *Biophysical Journal*, 101(7):1597–1603, 10 2011.

[23] Gijsje H Koenderink, Zvonimir Dogic, Fumihiko Nakamura, Poul M Bendix, Frederick C MacKintosh, John H Hartwig, Thomas P Stossel, and David A Weitz. An active biopolymer network controlled by molecular motors. *Proceedings of the National Academy of Sciences of the United States of America*, 106(36):15192–15197, 09 2009.

[24] O. Lieleg and A. R. Bausch. Cross-linker unbinding and self-similarity in bundled cytoskeletal networks. *Phys. Rev. Lett.*, 99:158105, Oct 2007.

[25] O. Lieleg, M. M. A. E. Claessens, Y. Luan, and A. R. Bausch. Transient binding and dissipation in cross-linked actin networks. *Phys. Rev. Lett.*, 101:108101, Sep 2008.

[26] O. Lieleg, K. M. Schmoller, M. M. A. E. Claessens, and A. R. Bausch. Cytoskeletal polymer networks: Viscoelastic properties are determined by the microscopic interaction potential of cross-links. *Biophysical Journal*, 96(11):4725–4732, 6 2009.

[27] Oliver Lieleg, Mireille M. A. E. Claessens, and Andreas R. Bausch. Structure and dynamics of cross-linked actin networks. *Soft Matter*, 6:218–225, 2010.

[28] Yi-Chia Lin, Chase P. Broedersz, Amy C. Rowat, Tatjana Wedig, Harald Herrmann, Frederick C. MacKintosh, and David A. Weitz. Divalent cations crosslink vimentin intermediate filament tail domains to regulate network mechanics. *Journal of Molecular Biology*, 399(4):637 – 644, 2010.

[29] J. Liu, G. H. Koenderink, K. E. Kasza, F. C. MacKintosh, and D. A. Weitz. Visualizing the strain field in semiflexible polymer networks: Strain fluctuations and nonlinear rheology of f-actin gels. *Phys. Rev. Lett.*, 98:198304, May 2007.

[30] John F. Marko and Eric D. Siggia. Stretching dna. *Macromolecules*, 28(26):8759–8770, 1995.

[31] Mirjam Mayer, Martin Depken, Justin S. Bois, Frank Julicher, and Stephan W. Grill. Anisotropies in cortical tension reveal the physical basis of polarizing cortical flows. *Nature*, 467(7315):617–621, 09 2010.

[32] David C. Morse. Viscoelasticity of concentrated isotropic solutions of semiflexible polymers. 2. linear response. *Macromolecules*, 31(20):7044–7067, 1998.

[33] Kei W. Müller, Robijn F. Bruinsma, Oliver Lieleg, Andreas R. Bausch, Wolfgang A. Wall, and Alex J. Levine. Rheology of semiflexible bundle networks with transient linkers. *Phys. Rev. Lett.*, 112:238102, Jun 2014.

[34] Michael P. Murrell and Margaret L. Gardel. F-actin buckling coordinates contractility and severing in a biomimetic actomyosin cortex. *Proceedings of the National Academy of Sciences*, 109(51):20820–20825, 2012.

[35] Guillaume Salbreux, Guillaume Charras, and Ewa Paluch. Actin cortex mechanics and cellular morphogenesis. *Trends in Cell Biology*, 22(10):536 – 545, 2012.

[36] Tim Sanchez, Daniel T. N. Chen, Stephen J. DeCamp, Michael Heymann, and Zvonimir Dogic. Spontaneous motion in hierarchically assembled active matter. *Nature*, 491(7424):431–434, 11 2012.

[37] Evan Spruijt, Joris Sprakel, Marc Lemmers, Martien A. Cohen Stuart, and Jasper van der Gucht. Relaxation dynamics at different time scales in electrostatic complexes: Time-salt superposition. *Phys. Rev. Lett.*, 105:208301, Nov 2010.

[38] Dimitrije Stamenovic. Cell mechanics: Two regimes, maybe three? *Nat Mater*, 5(8):597–598, 08 2006.

[39] Cornelis Storm, Jennifer J. Pastore, F. C. MacKintosh, T. C. Lubensky, and Paul A. Janmey. Nonlinear elasticity in biological gels. *Nature*, 435(7039):191–194, 05 2005.

[40] R. Tharmann, M. M. A. E. Claessens, and A. R. Bausch. Viscoelasticity of isotropically cross-linked actin networks. *Phys. Rev. Lett.*, 98:088103, Feb 2007.

[41] Andrea Vanossi, Nicola Manini, Michael Urbakh, Stefano Zapperi, and Erio Tosatti. *Colloquium* : Modeling friction: From nanoscale to mesoscale. *Rev. Mod. Phys.*, 85:529–552, Apr 2013.

[42] D.H. Wachsstock, W.H. Schwarz, and T.D. Pollard. Cross-linker dynamics determine the mechanical properties of actin gels. *Biophysical Journal*, 66(3, Part 1):801 – 809, 1994.

[43] Andrew Ward, Feodor Hilitski, Walter Schwenger, David Welch, A. W. C. Lau, Vincenzo Vitelli, L. Mahadevan, and Zvonimir Dogic. Solid friction between soft filaments. *Nat Mater*, advance online publication:–, 03 2015.

[44] Sabine M. Volkmer Ward, Astrid Weins, Martin R. Pollak, and David A. Weitz. Dynamic viscoelasticity of actin cross-linked with wild-type and disease-causing mutant -actinin-4. *Biophysical Journal*, 95(10):4915 – 4923, 2008.

[45] Jan Wilhelm and Erwin Frey. Elasticity of stiff polymer networks. *Phys. Rev. Lett.*, 91:108103, Sep 2003.

[46] M. Wyart, H. Liang, A. Kabla, and L. Mahadevan. Elasticity of floppy and stiff random networks. *Phys. Rev. Lett.*, 101:215501, Nov 2008.

[47] Norman Y. Yao, Daniel J. Becker, Chase P. Broedersz, Martin Depken, Frederick C. MacKintosh, Martin R. Pollak, and David A. Weitz. Nonlinear viscoelasticity of actin transiently cross-linked with mutant -actinin-4. *Journal of Molecular Biology*, 411(5):1062 – 1071, 2011.